

Petrographical and Geochemical Characteristics of Felsic Volcanic Rocks in the Upper Part of The Khorat Plateau, Thailand

VIMOLTIP SINGTUEN and THATCHAPON SEELA

Department of Geotechnology, Faculty of Technology, Khon Kaen University, Khon Kaen 40002 Thailand

Corresponding author: vimoltipst@gmail.com

Manuscript received: April, 19, 2024; revised: October, 05, 2024;
approved: July, 23, 2025; available online: August, 14, 2025

Abstract - The felsic volcanic rocks distributed in the western part of Nong Khai and Udon Thani Provinces are part of The Loei-Phetchabun Volcanic Belt. This study aims to investigate the petrography and geochemical characteristics of felsic volcanic rocks to classify specific names of rocks and explain their occurrences. The textures and compositions by petrographic analysis classify the studied rocks into four types: (1) rhyolite porphyry, (2) crystal tuff, (3) eutaxitic rhyolite porphyry, and (4) hornblende-biotite diorite. In addition, the total alkaline versus silica ($\text{Na}_2\text{O}+\text{K}_2\text{O}/\text{SiO}_2$) ratios classify these rocks into rhyolite, dacite, and basaltic andesite/diorite intrusion. Moreover, the major oxides and trace elements indicate that these volcanic rocks were generated from tholeiitic, transitional, and calc-alkaline magma series that formed along volcanic arcs. Therefore, the subduction of at least two tectonic terranes in the area may lead to the formation of the volcanic arc (felsic volcanic rocks and hornblende-biotite diorite).

Keywords: rhyolite, dacite; basaltic andesite, diorite, tuff, volcanic arc, tholeiitic series, calc-alkaline

© IJOG - 2025

How to cite this article:

Singtuen, V. and Seela, T., 2025. Petrographical and Geochemical Characteristics of Felsic Volcanic Rocks in the Upper Part of The Khorat Plateau, Thailand. *Indonesian Journal on Geoscience*, 12 (2), p.231-248. DOI: [10.17014/ijog.12.2.231-248](https://doi.org/10.17014/ijog.12.2.231-248)

INTRODUCTION

Background

Thailand's geological composition is characterized by the juxtaposition of continental blocks, notably The Indochina Terrane to the east and The Sibumasu Terrane to the west (Metcalfe, 2006; 2011). These Terranes are demarcated by The Sukhothai Fold Belt and The Loei Fold Belt. Within this region, a diverse array of geological structures and rock types is evident, encompassing sedimentary, metamorphic, volcanic, and intrusive formations, with a notable prevalence of rhyolites (Figure 1).

The western regions of Udon Thani Province and Nong Khai Province are encompassed within the geological formation known as The Loei Fold Belt, characterized by a mixture of igneous, sedimentary, and metamorphic rocks (Kamvong and Zaw, 2009; Khositanont *et al.*, 2013; Kamvong *et al.*, 2014; Salam *et al.*, 2014; Qian *et al.*, 2015; Nualkhao *et al.*, 2018). Specifically, the western expanse of these provinces exhibits a significant presence of volcanic rocks, which are attributed to the broader Loei-Phetchabun Volcanic Belt, situated within the eastern Loei subbelt (Qian *et al.*, 2015). The terrain in this area predominantly features north-south oriented

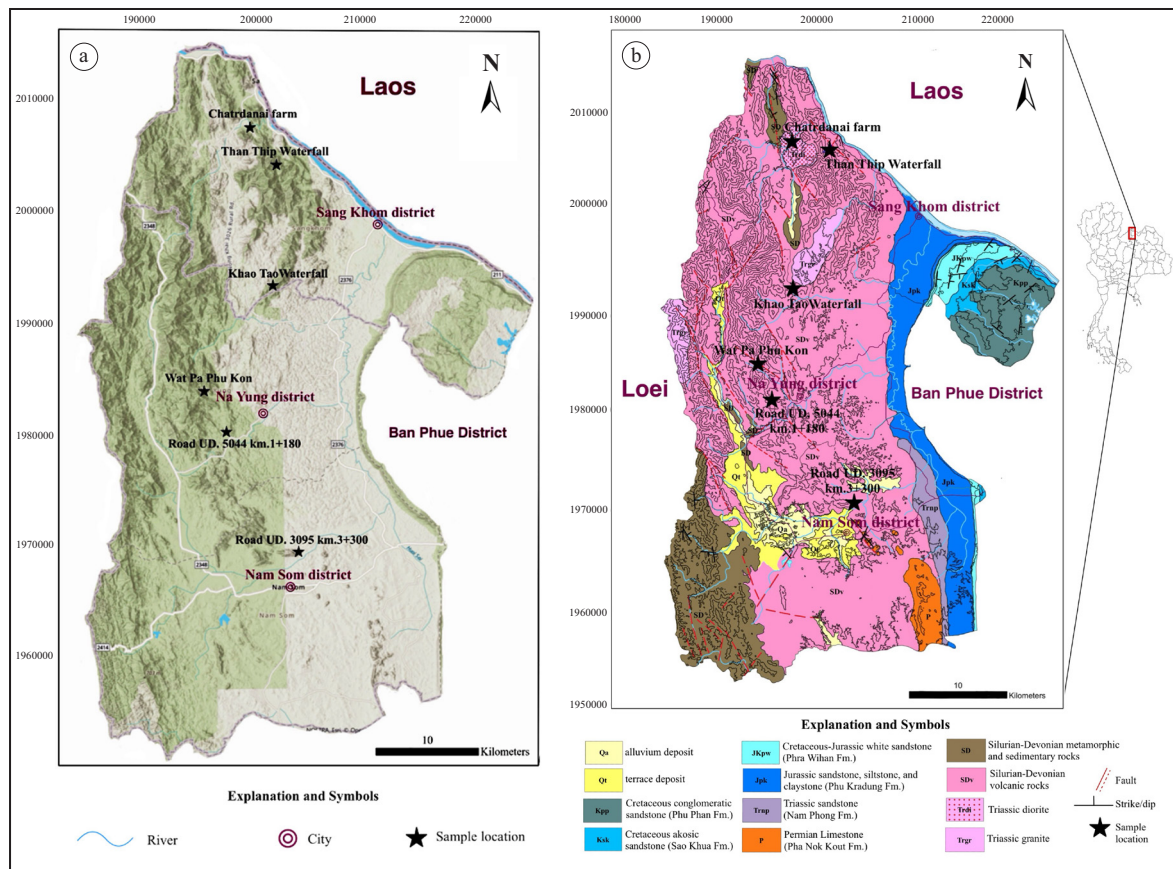


Figure 1. Geomorphic settings of the studied site; a). Location of the studied site (black star) with topographic characteristics and Mekong River in the north; b). Geologic setting of the studied site (geological data modified from DMR, 2007).

high mountains interspersed with sloped regions. Geological investigations reveal a predominance of Permian-Triassic era igneous formations comprising volcanic materials such as ash, tuff, rhyolite, and andesite, alongside intrusive igneous rocks like granite, granodiorite, diorite, and quartz monzonite (DMR, 2007). Using the U-Pb isotope method, the age determination of rhyolite and dacite rocks suggests their formation during the Silurian period (Khositanont *et al.*, 2013).

Despite efforts to survey research endeavors within the area, a comprehensive investigation into the volcanic rock formations is to be completed. Consequently, a scholarly impetus exists to undertake a detailed examination of the rocks within this locale. This study aims to scrutinize the petrology, formations, and geochemical attributes of volcanic rocks in the designated region. The acquired data will undergo meticulous analysis to elucidate the genesis and nomenclature of rocks within the

studied area, thereby augmenting the existing literature on rock formations and the geochemistry of volcanic rocks within the eastern Loei Subbelt.

Geological Settings

The elevation of Udon Thani Province averages around 140 m above mean sea level. To the west, the terrain is dominated by the Phetchabun Mountain range, characterized by a series of contiguous peaks running along the province border from Nam Som District southward. Conversely, the eastern region lies upon The Khorat Plateau, featuring dispersed low-lying mountains, with the Phu Phan Mountain Range standing out as a significant topographical feature (Figure 1a). The landscape gradually slopes towards the north, leading to The Mekong River, which delineates the northern boundary of The Khorat Plateau. The highest peak in the vicinity is Phu Luang, located in Loei Province, soaring approximately

1,571 m above mean sea level (DMR, 2009a; 2009b).

During the Late Permian to Early Triassic period, approximately 250 Ma, Thailand underwent a phase of heightened volcanic activity, forming in the formation of volcanic rocks across various regions (Intasopa and Dunn, 1994; Panjasawatwong *et al.*, 2006; Boonsoong *et al.*, 2011; Kamvong *et al.*, 2014; Salam *et al.*, 2014; Zhao *et al.*, 2016). In Udon Thani Province, these volcanic formations are categorized as part of the central volcanic belt extending eastward from Loei Province into The Nam Som District. Predominantly composed of calcareous rhyolite, tuff, and volcanic pebbles in shades ranging from light pink to purplish-grey and grey-brown (Figure 1b), these rocks originated during the Permo-Triassic period, forming as arch-shaped islands (DMR, 2009a; 2009b). However, previous analyses of volcanic rocks, including dacite and rhyolite, coupled with U-Pb isotope dating, revealed ages of 425 ± 7 Ma and 433 ± 10 Ma, respectively, suggesting formation during the Silurian period (Khositanont *et al.*, 2013). Additionally, Rb-Sr isotopic analysis indicates volcanic activity during the Late Devonian to Carboniferous period (374 to 361 Ma), further correlating with regional tectonic processes, particularly the subduction of The Sukhothai Terrane beneath the Indochina Terrane (Intasopa and Dunn, 1994).

Intrusive igneous rocks, formed through the gradual crystallization of magma deep beneath the earth crust, are prevalent in Nam Som District and Na Yung Districts. These rocks feature a range of compositions from granite to granodiorite, diorite, and hornblendite. These rocks often intersect with volcanic formations, forming intrusive walls within the volcanic rock units. Notably, the age of intrusive igneous rocks aligns with the Permo-Triassic period, approximately 230 million years ago (DMR, 2009a; 2009b).

In Loei Province and surrounding regions, situated at the northwestern margin of The Khorat Plateau, volcanic rocks exhibit a predominant north-south orientation. These rocks can be categorized into two main groups based on age: Devonian-Carboniferous rocks, distributed

within a confined area, and volcanic rocks from the Permian-Triassic period, dispersed across a wider expanse.

The Devonian-Carboniferous volcanic rocks, primarily comprising rhyolite, are prevalent in the eastern vicinity of Pak Chom District, Sangkhom District, and Nam Som District, or along the northwestern edge of The Khorat Plateau. These formations predominantly consist of rhyolite and rhyolitic rocks, with occasional occurrences of andesite. The relative age of this rock group, determined through isotope dating methods, corresponds to the Devonian-Carboniferous period (DMR, 2007).

Rhyolite formations exhibit a fine-grained to microcrystalline texture, often displaying mineral structures known as "porphyritic textures," characterized by quartz crystals ranging from 0.1 to 4 mm in size, sanidine and plagioclase crystals measuring approximately 0.2 to 2 mm, and a groundmass composed of felsic minerals (quartz, K-feldspar, and plagioclase) and fine-sized spherulites (Intasopa and Dunn, 1994).

Studies conducted by Khositanont *et al.* (2013) on felsic volcanic rocks in the eastern Loei Subbelt revealed geochemical characteristics indicative of a calc-alkaline magma series. These rocks are associated with island arc and syn-subduction tectonics, with U-Pb zircon dating indicating formation between 434 to 435 Ma or Early Silurian period (Khositanont *et al.*, 2013). This geological activity may be linked to the subduction of South China beneath Indochina from the west. The Silurian arc-related rhyolites on the western edge of the Indochina Block reflects formation resulting from the subduction of The Proto-Tethys Oceanic Plate beneath The Indochina Block, occurring prior to The Devonian Loei Ocean opening (~ 361 Ma) (Intasopa and Dunn, 1994).

Furthermore, U-Pb isotope dating of intrusive igneous rocks in The Phu Lon area suggests that diorite rocks are approximately 240.6 ± 1.2 Ma (Nie *et al.*, 2019), while monzonite rocks date back to around 244 ± 4 Ma (Kamvong and Zaw, 2009), corresponding to the Middle Triassic period.

METHODS AND MATERIALS

The methodology employed in this study comprises bibliometric analysis, field observation, petrography, geochemical analysis (involving major and trace element analyses), discussion, and conclusion.

Field surveys and data collection involved gathering information on rock outcrops and their characteristics, including colour, texture, mineral composition, and degree of weathering. Approximately five to six representative samples were collected from six designated studied sites (Table 1), which consists of Than Thip Waterfall (sample code: TT), Rai Chatdanai Café (sample code: CD), Khao Tao Waterfall (sample code: KT), Wat Pa Phu Kon (sample code: PK), Rural Highway UD. 5044 km 1+180 (sample code: NY), and Rural Highway UD. 3095 km 3+300 (sample code: NS) as shown in Figure 2. Notably, the NY-01 sample contains large xenoliths (X), which are more easily observable and analyzable compared to those in other samples. Consequently, NY-02(X) and NY-03(X) represent large xenoliths within the NY-01 sample.

Thin sections of rock were prepared with a thickness of 0.03 mm and examined under a polarized light microscope (Nikon ECLIPSE Ci-POL) to analyze rock texture and mineral components. Mineral quantities were then quantified as a percentage by volume to classify the specific rock types at each studied point (Figure 3).

The geochemical analysis of rock powder samples was performed using a Portable X-ray Fluorescence (pXRF) analyzer (Olympus Vanta model) at The Department of Geotechnology, Faculty of Technology, Khon Kaen University

(Table 2). This analysis aimed to determine the types and concentrations of major and trace elements in the rocks, aiding in their classification into specific rock types. To ensure reliable results, the pXRF measurements were conducted on smooth, fresh surfaces of the rock samples. Given the limitations of the pXRF instrument in accurately detecting trace amounts of Na, the Na values were combined with K to calculate the total alkali content. This methodological adjustment aligns with prior studies on rhyolite geochemistry (Intasopa and Dunn, 1994; Zhao *et al.*, 2016).

Rock classification will be based on major oxides, the total alkali-silica ratio (Le Bas *et al.*, 1986), and trace elements, specifically the Zr/Ti and Nb/Y ratios (Winchester and Floyd, 1977). Volcanic rocks typically originate from four well-established magma series: tholeiitic, alkaline, calc-alkaline, and shoshonitic (Jakes and White, 1969; 1970; 1972). The classification of magma series is primarily achieved using correlation-based diagrams that focus on major oxide compositions, such as the combined sodium oxide (Na_2O) and potassium oxide (K_2O) content relative to silicon dioxide (SiO_2) (Irvine and Baragar, 1971). Additionally, trace element discrimination diagrams, particularly the Y-Zr diagram (MacLean and Barrett, 1993) and the Nb+Y versus Rb diagram (Pearce *et al.*, 1984), are commonly employed to further refine the classification.

Subsequently, the results obtained from the petrographic and geochemical analyses will be employed to discuss the classification and spatial distribution of volcanic rocks, ultimately leading to the interpretation of the associated tectonic processes.

Table 1. Location of The Studied Areas and Sampling in Nong Khai and Udon Thani Provinces

Province	Location	UTM	Sample Code
Nong Khai	Than Thip Waterfall	48Q 202152E 2006164N	TT
	Chatrdanai Farm Café	48Q 198992E 2008994N	CD
	Khao Tao Waterfall	48Q 200613E 1993853N	KT
Udon Thani	Wat Pa Phu Kon	48Q 195320E 1983701N	PK
	road UD. 5044 km.1+180	48Q 196385E 1980993N	NY
	road UD. 3095 km.3+300	48Q 203321E 0970212N	NS

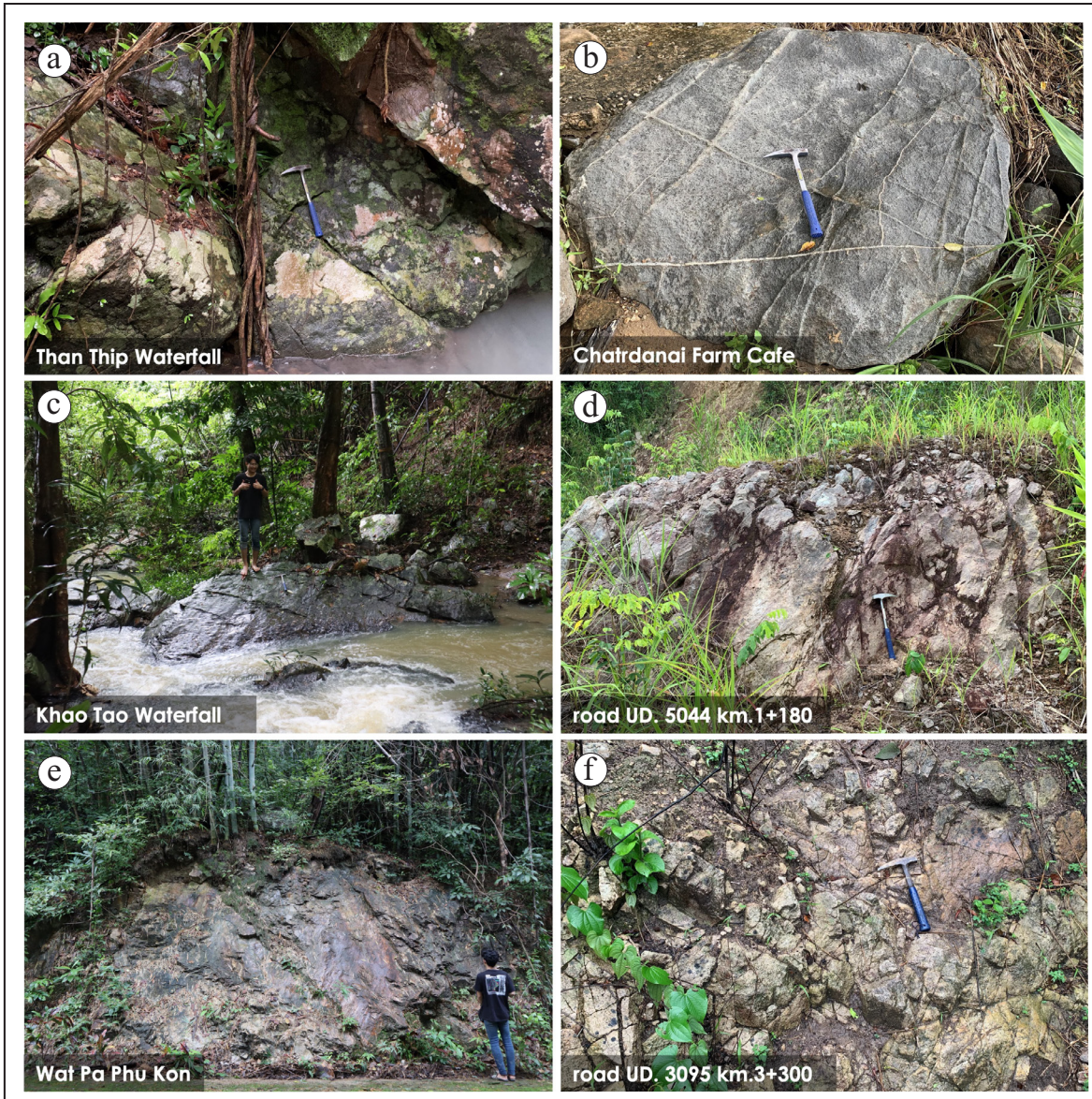


Figure 2. Outcrop characteristics; a). felsic volcanic rocks (rhyolite and tuff) at Than Thip Waterfall exhibit parallel jointing; b). mafic intrusion with quartz vein at Chatrdanai Farm Café; c). rhyolites at Khao Tao Waterfall present parallel jointing; d). tuffaceous rocks at Rural Road UD.5044 km. 1+180 display signs of alteration and multiphase jointing; e). rhyolite at Wat Pa Phu Kon exhibits slickensides; and f). rhyolite at Rural Road UD.3095 km. 3+300 demonstrates multiphase jointing.

RESULTS

Lithology

Through field surveys, rocks have been categorized into three primary groups: rhyolite porphyry, tuff, and diorite (Figure 2). Rhyolite porphyry is distributed across areas including Than Thip Waterfall, Nam Tao Khao Tao, Wat Pa Phu Kon, and the rural road UD. 3095 km 3+300 (Figures 1 and 2). These samples exhibit weathered brown surface colour, transitioning to

grey, greenish-grey, purple-grey, and pink colours upon fresh exposure.

The samples exhibit a porphyritic texture, characterized by microphenocrysts primarily composed of fine-grained quartz and feldspar (less than 1 mm in size). Additionally, some samples contain epidote as a secondary mineral, present both as alteration phases and within veins (Figures 2a and 2f). Tuff formations are distributed around Than Thip Waterfall and Rural Highway UD. 5044 at kilometer 1+180. These rocks

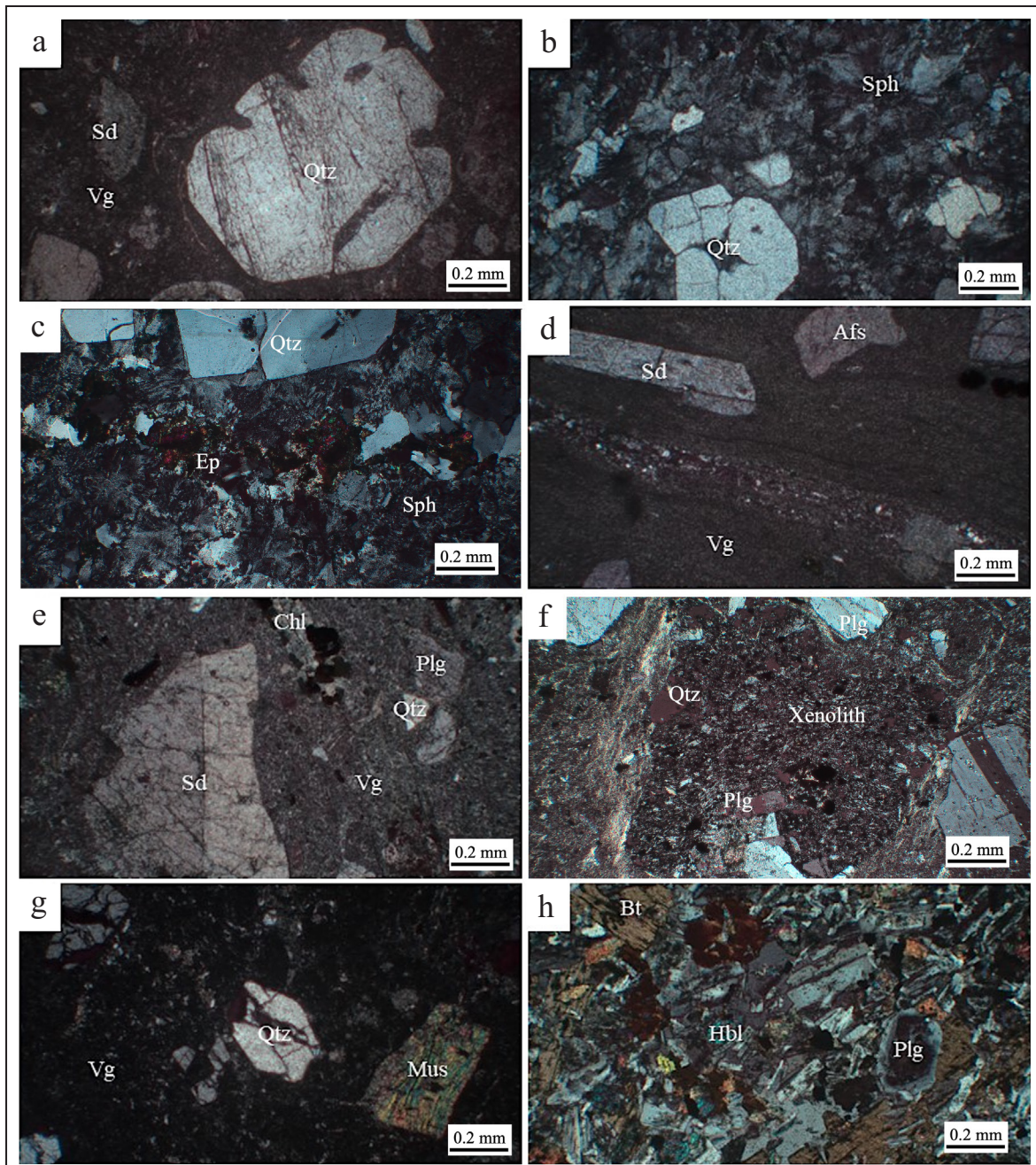


Figure 3. Photomicrographs of the studied rocks; a). rhyolite porphyry; b). quartz in rhyolite display hollow and embayed characteristics; c). quartz phenocryst, spherulite, and epidote in rhyolite; d). Eutaxitic rhyolite porphyry; e). sanidine phenocryst in eutaxitic rhyolite porphyry; f). dacite xenolith in volcanic rocks; g). crystal tuff; and h). hornblende-biotite diorite. Abbreviations of minerals names: Qtz = quartz; Sd = sanidine; Plg = plagioclase; Mus = muscovite; Afs = alkaline feldspar; Bt = biotite; Hbl = hornblende; Chl = chlorite; Ep = epidote; Vg = volcanic glass; Sph = spherulite (Whitney and Evans, 2010).

display a weathered brown exterior, transitioning to a fresh purple-red-black hue.

The rocks exhibit a combination of pyroclastic textures, containing fine-grained quartz and feldspars within a very fine-grained groundmass. Coarse-grained to very coarse-grained felsic rock

fragments (approximately 1 to 3 cm) occur as lapilli. The texture, dominated by dark volcanic glass and felsic minerals, is fine-grained and difficult to distinguish with the naked eyes.

Diorite occurrences are identified around The Rai Chattanai Café, characterized by a greyish-

**Petrographical and Geochemical Characteristics of Felsic Volcanic Rocks
in the Upper Part of The Khorat Plateau, Thailand (V. Singtuen and T. Seela)**

Table 2. Geochemical Data of Felsic Volcanic Rocks, Xenoliths, and Mafic Intrusions

Sample	TT-01	TT-02	TT-03	KT-01	KT-02	KT-03
Rock	rhyolite porphyry	crystal tuff	eutaxitic rhyolite porphyry	rhyolite porphyry	eutaxitic rhyolite porphyry	eutaxitic rhyolite porphyry
Major Oxides (%)						
MgO	-	-	-	-	-	-
Al ₂ O ₃	15.4075	13.2965	13.4300	14.3941	16.6193	16.7794
SiO ₂	76.1780	72.6448	76.9028	76.1538	74.0540	75.3123
P ₂ O ₅	-	-	0.0841	-	0.0223	0.1197
SO ₃	0.0532	0.0971	0.1401	0.0541	0.0283	0.1580
CaO	0.2339	4.6906	0.5330	1.1591	1.8443	1.5757
TiO ₂	0.2107	0.1584	0.1719	0.1146	0.2319	0.2869
MnO	-	0.0653	0.1154	0.0578	0.1541	0.1277
FeO	0.8041	2.3363	1.7570	1.7244	1.7600	1.6900
NiO	0.0029	-	-	-	-	-
Total alkaline*	7.1096	6.7110	6.8659	6.3420	5.2860	3.9504
Trace Element (ppm)						
V	-	-	-	-	-	-
Cr	-	30.333	-	-	-	-
Co	-	-	-	-	-	-
Cu	-	5.000	-	8.500	6.500	-
Zn	23.000	51.333	26.000	25.500	67.000	65.000
As	6.500	-	8.500	-	-	-
Se	1.500	-	-	2.000	-	-
Rb	157.500	154.667	148.500	133.000	110.500	94.000
Sr	59.000	83.667	63.000	105.500	173.000	143.000
Y	49.500	38.000	51.500	28.500	34.500	38.000
Zr	91.000	122.667	99.500	138.000	219.000	230.000
Nb	1.000	1.000	1.000	3.000	3.500	8.000
Mo	5.000	2.333	-	4.000	6.000	-
Ag	-	-	-	-	-	-
Cd	-	-	-	10.500	-	-
Sn	16.500	11.333	-	26.500	43.500	-
Sb	-	-	-	-	22.000	-
Ba	395.500	343.333	1130.500	487.000	348.500	-
La	-	-	-	-	-	-
Ce	51.500	-	54.000	53.500	61.000	-
Pr	-	-	-	-	-	-
Nd	-	-	-	-	-	-
W	-	-	-	-	-	-
Hg	-	-	-	-	-	-
Pb	5.500	15.333	28.500	11.000	16.500	11.000
Bi	-	-	-	-	-	-
Th	23.000	14.333	22.000	17.500	30.000	-
U	-	-	-	-	-	-

*Total alkaline = K₂O+Na₂O

Table 2. Geochemical Data of Felsic Volcanic Rocks, Xenoliths, and Mafic Intrusions (continue)

Sample	KT-04	NY-01	NY-02 (X)	NY-03 (X)	PK-01	PK-02
Rock	rhyolite porphyry	crystal tuff	dacite	dacite	eutaxitic rhyolite porphyry	eutaxitic rhyolite porphyry
Major Oxides (%)						
MgO	-	-	-	-	-	-
Al ₂ O ₃	13.0646	13.0485	24.2465	24.6800	4.1111	16.8143
SiO ₂	75.1206	72.0526	64.8106	63.9373	94.7505	76.7385
P ₂ O ₅	-	0.0527	0.4635	0.2813	-	0.0257
SO ₃	0.1102	0.0290	-	0.0740	0.0487	-
CaO	1.8606	0.5293	0.3246	0.2353	0.0546	0.0995
TiO ₂	0.1453	0.4906	0.6238	0.4842	0.1248	0.0658
MnO	0.0431	0.4305	0.0803	0.1432	0.0144	0.0153
FeO	1.7592	5.8763	4.1074	4.0545	0.1499	0.6999
NiO	-	0.0028	0.0095	0.0051	-	-
Total alkaline*	7.8963	7.4876	5.3337	6.1052	0.7460	5.5410
Trace Element (ppm)						
V	-	-	-	-	-	-
Cr	-	-	174.000	254.000	-	-
Co	-	-	-	-	-	-
Cu	-	21.000	26.000	-	-	11.500
Zn	25.000	93.000	37.000	53.000	4.000	10.500
As	-	16.000	-	-	-	-
Se	-	-	-	-	2.000	-
Rb	154.000	134.000	56.000	66.000	7.500	62.500
Sr	54.000	319.000	739.000	622.000	4.500	16.500
Y	30.000	29.000	109.000	88.000	11.500	13.000
Zr	98.000	202.000	136.000	124.000	68.500	93.000
Nb	6.000	0.500	0.500	0.500	5.000	7.000
Mo	-	-	-	-	5.000	-
Ag	-	-	-	-	12.500	-
Cd	-	-	-	-	-	-
Sn	-	-	46.000	40.000	-	24.000
Sb	-	-	-	-	35.500	37.000
Ba	536.000	1047.000	2005.000	1792.000	-	76.500
La	-	84.000	-	-	-	-
Ce	-	-	-	-	-	-
Pr	-	-	-	-	-	-
Nd	194.000	295.000	-	-	-	-
W	-	-	-	-	-	-
Hg	-	-	-	-	-	-
Pb	15.000	30.000	9.000	10.000	3.500	8.000
Bi	-	-	-	-	-	-
Th	26.000	18.000	-	21.000	-	9.000
U	6.000	-	-	-	-	-

*Total alkaline = K₂O+Na₂O
X (xenolith)

**Petrographical and Geochemical Characteristics of Felsic Volcanic Rocks
in the Upper Part of The Khorat Plateau, Thailand (V. Singtuen and T. Seela)**

Table 2. Geochemical Data of Felsic Volcanic Rocks, Xenoliths, and Mafic Intrusions in The Northern Khorat Plateau, Thailand (continue)

Sample	PK-03	NS-01	NS-02	NS-03	CD-01	CD-02
Rock	eutaxitic rhyolite porphyry	Rhyolite Porphyry	Rhyolite Porphyry	Rhyolite Porphyry	hornblende-biotite diorite	hornblende-biotite diorite
Major Oxides (%)						
MgO	-	-	-	-	2.5498	2.7332
Al ₂ O ₃	9.2515	25.0944	21.9004	20.6229	17.9237	17.8935
SiO ₂	86.7052	65.3500	69.0614	70.0559	54.0630	52.5397
P ₂ O ₅	-	-	-	-	0.3979	0.4435
SO ₃	0.0494	0.0594	0.2018	0.0776	-	-
CaO	0.0635	0.1486	0.2267	0.0944	9.7584	10.4571
TiO ₂	0.0897	0.1686	0.2087	0.1604	1.7545	1.5555
MnO	-	0.0170	0.0311	0.0346	0.1740	0.1760
FeO	0.5921	2.2377	1.6190	1.8537	9.7380	10.4770
NiO	-	-	-	-	-	0.0024
Total alkaline*	3.2486	6.9244	6.7509	7.1004	3.6407	3.7220
Trace Element (ppm)						
V	-	-	-	-	299.000	286.000
Cr	-	105.000	-	-	-	51.000
Co	-	-	-	-	-	72.000
Cu	15.000	-	17.500	7.000	28.000	35.500
Zn	-	33.000	30.000	41.000	95.000	86.500
As	-	-	-	2.500	-	-
Se	3.000	5.000	2.500	-	-	-
Rb	40.000	128.000	116.500	121.000	73.000	71.500
Sr	18.000	8.000	19.500	14.500	979.000	1161.000
Y	10.000	15.000	13.500	15.500	24.000	20.000
Zr	66.000	85.000	70.500	77.000	117.000	105.500
Nb	5.000	1.000	1.000	2.000	3.000	3.000
Mo	-	-	4.500	5.500	-	-
Ag	-	-	-	2.000	-	-
Cd	28.000	-	-	-	-	-
Sn	48.000	-	-	17.000	46.000	37.000
Sb	-	-	-	-	72.000	-
Ba	-	-	1847.500	557.500	-	257.500
La	-	-	-	-	-	-
Ce	-	-	-	109.500	-	-
Pr	-	-	-	71.000	-	-
Nd	-	-	-	-	-	-
W	-	-	-	-	-	-
Hg	-	-	-	-	-	-
Pb	8.000	-	10.000	7.500	15.000	6.000
Bi	-	-	-	-	-	-
Th	-	-	9.500	27.500	-	11.000
U	-	-	-	3.000	-	-

*Total alkaline = K₂O+Na₂O

brown weathered surface and a fresh greyish appearance. These samples are composed of feldspar, hornblende, and biotite, exhibiting a fine-grained equigranularity texture. In some areas, mafic intrusions are observed cutting through the felsic volcanic rocks.

Petrography

Petrography was examined on twelve samples from six locations. These samples were classified into four distinct groups based on their rock texture and mineral composition under microscopic analysis: (1) four samples of rhyolite, (2) three samples of crystal tuff, (3) four samples of rhyolite exhibiting lava flows, and (4) one sample of hornblende-biotite diorite (Figure 3).

Rhyolite porphyry (samples TT-01, KT-01, KT-04, NS-01, NS-02, and NS-03) exhibits a distinctive porphyritic texture characterized by a combination of crystals and glass (hypocrystalline) as shown in Figures 3a and 3b. This composition features two crystal sizes (inequigranular), with phenocrysts comprising 35-45 modal % of the rock mass. These phenocrysts, measuring between 0.10 and 2.00 mm, are primarily composed of quartz, sanidine, and opaque minerals (Figure 3a), along with a minor presence of plagioclase and muscovite. Quartz crystals display hollow and embayed characteristics (Figure 3b). The groundmass comprises volcanic glass that has undergone partial devitrification, transforming into quartz and alkaline feldspar. Additionally, spherulites (0.20-0.60 mm) and epidote are observed as shown in Figure 3c.

Eutaxitic rhyolite porphyry (samples TT-03, KT-02, KT-03, PK-01, PK-02, and PK-03) presents an eutaxitic texture, wherein crystals and glass (hypocrystalline) are intermingled. Like rhyolite porphyry, this rock exhibits two crystal sizes, with inequigranular phenocrysts accounting for 30-45 modal % of the composition (Figure 3d). These phenocrysts, ranging from 0.10 to 2.00 mm, primarily include quartz, plagioclase, potassium feldspar, and opaque minerals (Figure 3e). Quartz crystals also demonstrate hollow and embayed features. The groundmass comprises volcanic glass, with some regions undergoing

devitrification into quartz, alkaline feldspars, and fine-sized plagioclase.

The dacite xenolith (samples NY-02(X) and NY-03(X)) observed in the volcanic rocks exhibits a porphyritic texture, characterized by plagioclase microphenocrysts measuring 0.1 to 0.2 mm (Figure 3f). The groundmass of the basalt is primarily composed of plagioclase, with minor amounts of quartz, clinopyroxene, and opaque minerals. The groundmass plagioclase displays a trachytic texture, indicating that this basalt likely originated from a lava flow.

Crystal tuff (samples TT-02, NY-01, NY-02, and NY-03) displays pyroclastic and fragmental textures, comprising a mixture of crystals and glass or hypocrystalline material. Inequigranular crystals encompass quartz (exhibiting hollow and swallowtail features), sanidine, plagioclase, epidote, chlorite, and opaque minerals, ranging from complete to subhedral crystals measuring 0.15 to 2.00 mm in size (Figure 3g). Volcanic glass fragments, measuring 0.20 to 0.60 mm, are also present. The rock fragments observed consist of mafic intrusive rocks and volcanic rocks (rhyolite, dacite, and andesite), measuring 1.00 to 1.20 mm. In addition, the NY samples exhibit mafic xenoliths (andesite-basalt) ranging in size from 5 to 10 cm.

The hornblende-biotite diorite (samples CD-01 and CD-02) exhibits a fine-grained equigranularity texture. This intrusive rock comprises holocrystalline material, the rock primarily consists of plagioclase, hornblende, biotite, and opaque minerals, ranging from 0.10 to 0.80 mm in size (Figure 3h). This intrusion displays a poikilitic texture, characterized by plagioclase chadacrysts within hornblende and biotite oikocrysts. More specifically, ophitic/subophitic texture is observed in samples, which have been interpreted as representing the shallow intrusion.

Geochemistry

The results of the geochemical analysis are presented in Table 2, delineating major oxides and trace elements. The major oxides can be classified into three groups: rhyolite, dacite, and basaltic andesite (or hornblende-biotite diorite; CD-01 and CD-02), based on the total alkali-silica ratio

(Figure 4a), which aligns with the classification derived from the Zr/Ti and Nb/Y ratios (Figure 4b). Moreover, the xenoliths (NY-02(X) and NY-03(X)) within the volcanic rocks (in NY-01 samples) can be classified as dacite, containing lower SiO₂ content compared to their host rock (rhyolite).

The chemical composition of rhyolite (sample codes: TT, KT, and PK) predominantly comprises the following major oxides: 72.05-94.75 wt.% SiO₂, 4.10-16.61 wt.% Al₂O₃, 0.74-7.90 wt.% K₂O, and Na₂O, 0.05-4.69 wt.% CaO, 0.06-0.49 wt.% TiO₂, 0.00-0.43 wt.% MnO, 0.59-5.87 wt.% FeO_{total}, with less than 0.26 wt.% MgO, and less than 0.12 wt.% P₂O₅.

In addition, dacite (sample codes: NY and NS) consists of the following major oxide compounds:

64.81-69.83 wt.% SiO₂, 20.52-24.67 wt.% Al₂O₃, 5.33-7.60 wt.% K₂O and Na₂O, 0.09-0.32 wt.% CaO, 0.16-0.62 wt.% TiO₂, 0.02-0.14 wt.% MnO, 1.62-4.12 wt.% FeO_{total} with less than 0.20 wt.% P₂O₅. This group exhibits the absence of MgO.

The chemical composition of basaltic andesite (diorite intrusion: samples CD-01 and CD-02) comprises the following main oxide compounds: 52.54-56.13 wt.% SiO₂, 2.07-2.73 wt.% MgO, 16.14-17.92 wt.% Al₂O₃, 3.26-3.72 % K₂O and Na₂O, 9.75-10.45 wt.% CaO, 1.32-1.75 wt.% TiO₂, 0.15-0.17 wt.% MnO, 9.73-10.47 wt.% FeO_{total} and 0.40-0.44 wt.% P₂O₅.

Harker-type variation diagrams of SiO₂ versus selected major and minor oxides (e.g. K₂O, Al₂O₃, Rb, Sr) exhibit negative correlations (Figure 5),

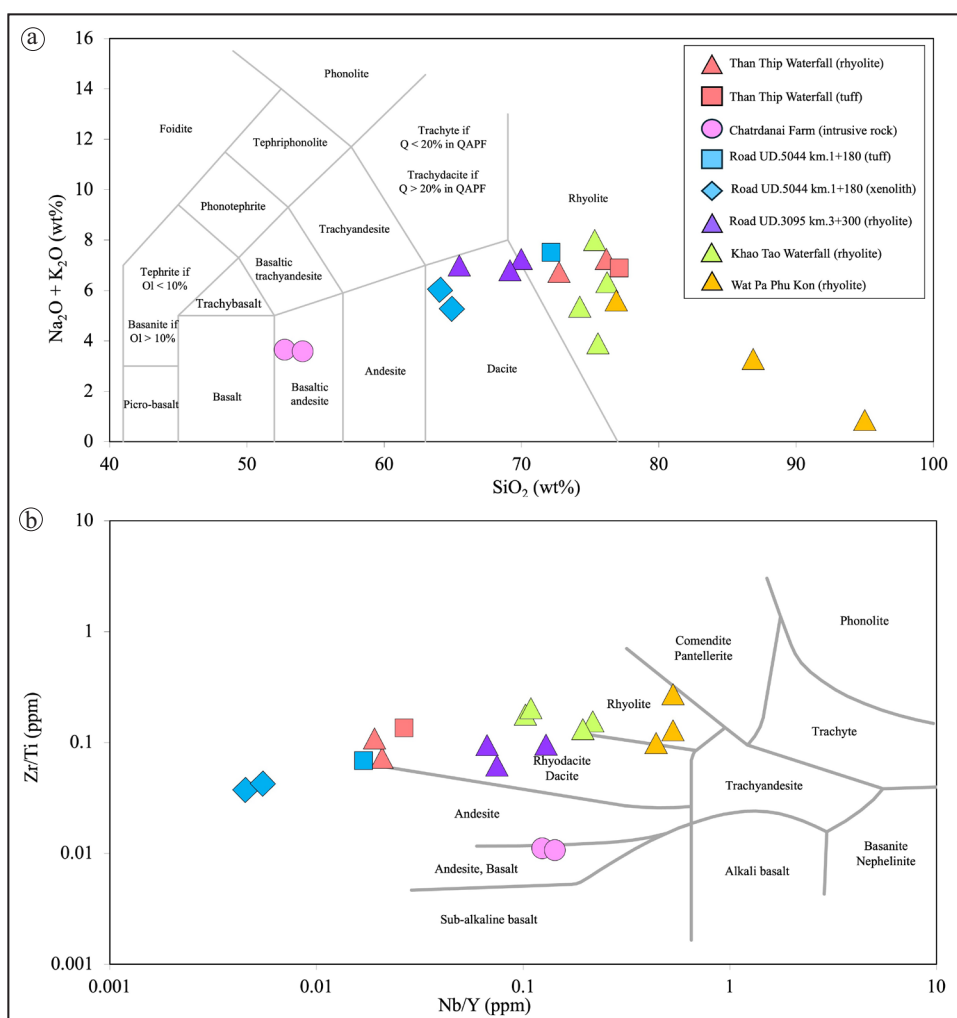


Figure 4. Rock name classification by geochemical analysis; a). Total Alkali-Silica (TAS) diagram for volcanic classification (diagram modified from Le Bas *et al.*, 1986); b). The ratio of Nb/Y and Zr/Ti classification (diagram modified from Winchester and Floyd, 1977)

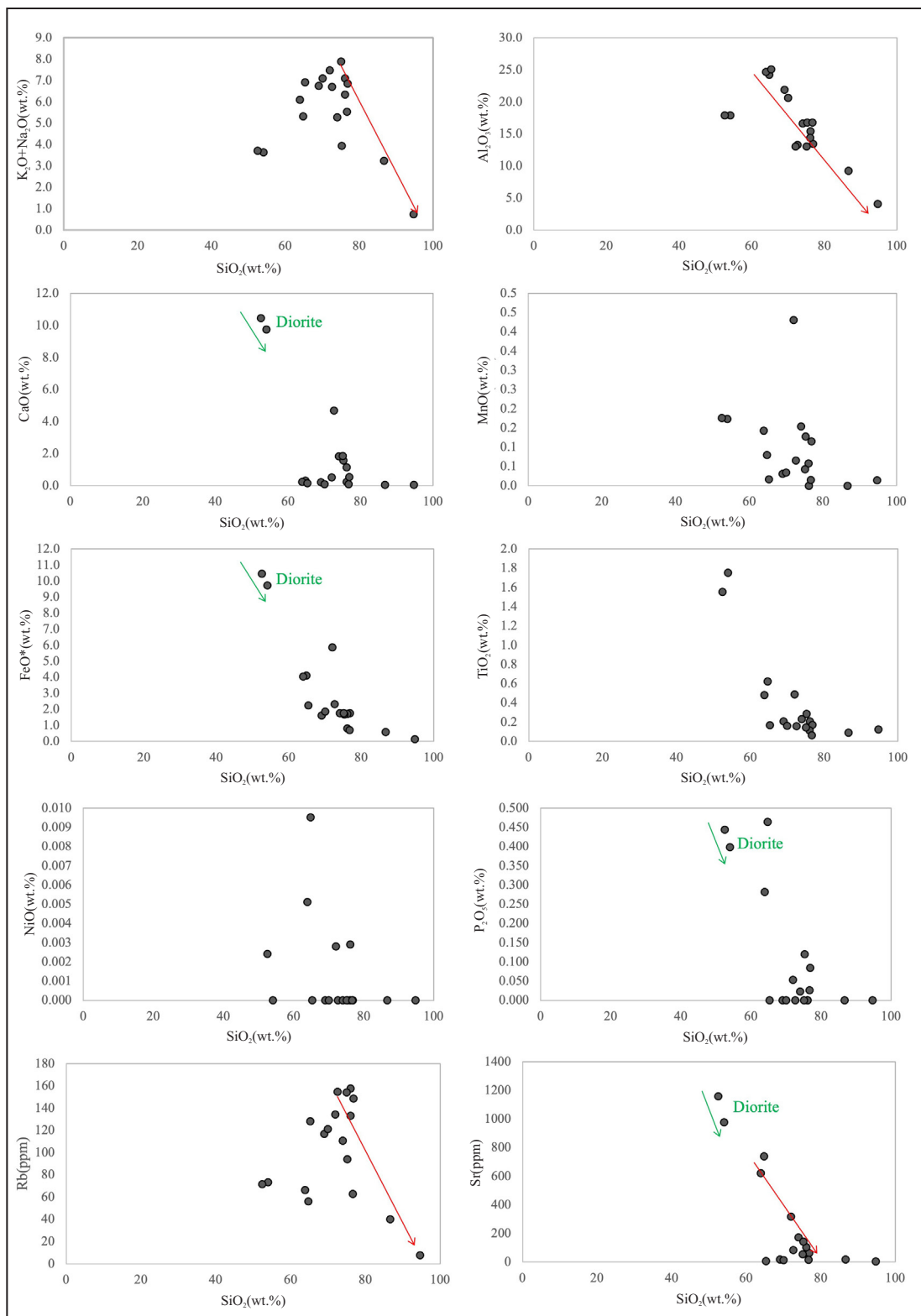


Figure 5. Harker diagrams plotting between SiO_2 versus major oxides, minor oxides, and trace elements.

indicating the crystallization of sanidine as phenocrysts within rhyolitic compositions. Furthermore, the observed negative trends suggest that

Rb and Sr can substitute for alkali elements in the sanidine structure. In contrast, CaO , MnO , FeO , MnO , NiO , TiO_2 , and P_2O_5 in rhyolite exhibit no

significant trends, rendering them less informative for geochemical interpretation in this context. In addition, the diorite samples exhibit negative correlations for CaO, Al₂O₃, MgO, FeO, P₂O₅, and Sr, indicating the crystallization of plagioclase, hornblende, and apatite in the mafic rocks. The observed trends also suggest that Sr can substitute for cations within these minerals.

Magma Series and Tectonic Discrimination

The magma compositions observed in this study fall within the sub-alkaline series, as determined using correlation-based magma series classification diagrams. These diagrams primarily focus on major oxide compositions, such as the combined sodium oxide (Na₂O) and potassium oxide (K₂O) content relative to silicon dioxide (SiO₂), as illustrated in Figure 6a.

The Y–Zr discrimination diagram (Figure 6b) indicates that the rhyolitic rocks and diorite from Rai Chattanai Café in the studied area were predominantly derived from a transitional magma series. However, exceptions include samples from Wat Pa Phu Kon (PK samples) and Rural Highway UD. 5044 (NY samples), which originated from a calc-alkaline magma series, and four additional samples from the Khao Tao (KT samples) and Than Thip Waterfalls (TT samples), which belong to the tholeiitic series.

The differences in magma series likely arise from variations in tectonic settings, magma sources, and evolutionary processes influenced by the tectonic and magmatic history of the region. The Chatrdanai Farm intrusion tholeiitic character suggests formation in a mantle-dominated extensional environment, while the calc-alkaline nature of The Khao Tao Waterfall rhyolite reflects subduction-related processes with significant crustal interaction.

Volcanic rocks and intrusive rocks occurring along volcanic arcs (involves assessing the correlation between the combined content of niobium (Nb) and yttrium (Y) with rubidium (Rb) as shown in Figure 6c, encompassing rock samples obtained from various sites: Than Thip Waterfall (TT samples), Khao Tao Waterfall (KT samples), Rai Chattanai (CD samples), Wat Pa Phu Kon

Studied Point (PK samples), Rural Highway UD. 5044 (NY samples) at kilometer marker 1+180, and Rural Highway UD. 3095 (NS samples) at kilometer marker 3+300. Volcanic rocks associated with intrusions within continental plates (within-plate), including xenolith collected from the studied point along Rural Highway UD. 5044 at kilometer marker 1+180 (xenolith within NY sample).

The observed differences in magma series likely reflect variations in tectonic settings, magma sources, and magmatic evolution. The transitional series indicates an intermediate tectonic environment, the calc-alkaline series suggests subduction-related processes, and the tholeiitic series points to extensional tectonics. These differences highlight the complex magmatic history of the studied area, shaped by diverse geological processes over time.

DISCUSSION

The petrographic and geochemical compositions of volcanic rocks in The Udon Thani and Nong Khai Provinces can be categorized into four distinct groups: (1) rhyolite porphyry characterized by quartz crystals with hollow interiors and swallow tails, along with sanidine, plagioclase, muscovite, and opaque minerals, (2) eutaxitic rhyolite porphyry comprised quartz, sanidine, plagioclase, and opaque minerals, (3) crystal tuff composed of quartz, sanidine, plagioclase, opaque minerals, chlorite, and epidote, with identified glass fragments and fragments of both intrusive and volcanic igneous rocks that defy classification, and (4) diorite containing plagioclase, hornblende, biotite, and opaque minerals. Rhyolite porphyry, eutaxitic rhyolite porphyry, and crystal tuff were classified as rhyolite based on geochemical analysis, while diorite was categorized as basaltic andesite. Additionally, xenoliths within the tuff were identified as dacite based on their geochemical composition.

In rhyolite, quartz exhibits distinctive features such as hollow interiors and embayed crystals (Figures 3a and 3b), which are not the result of mineral melting but rather a consequence of rapid magma cooling triggered by sudden pres-

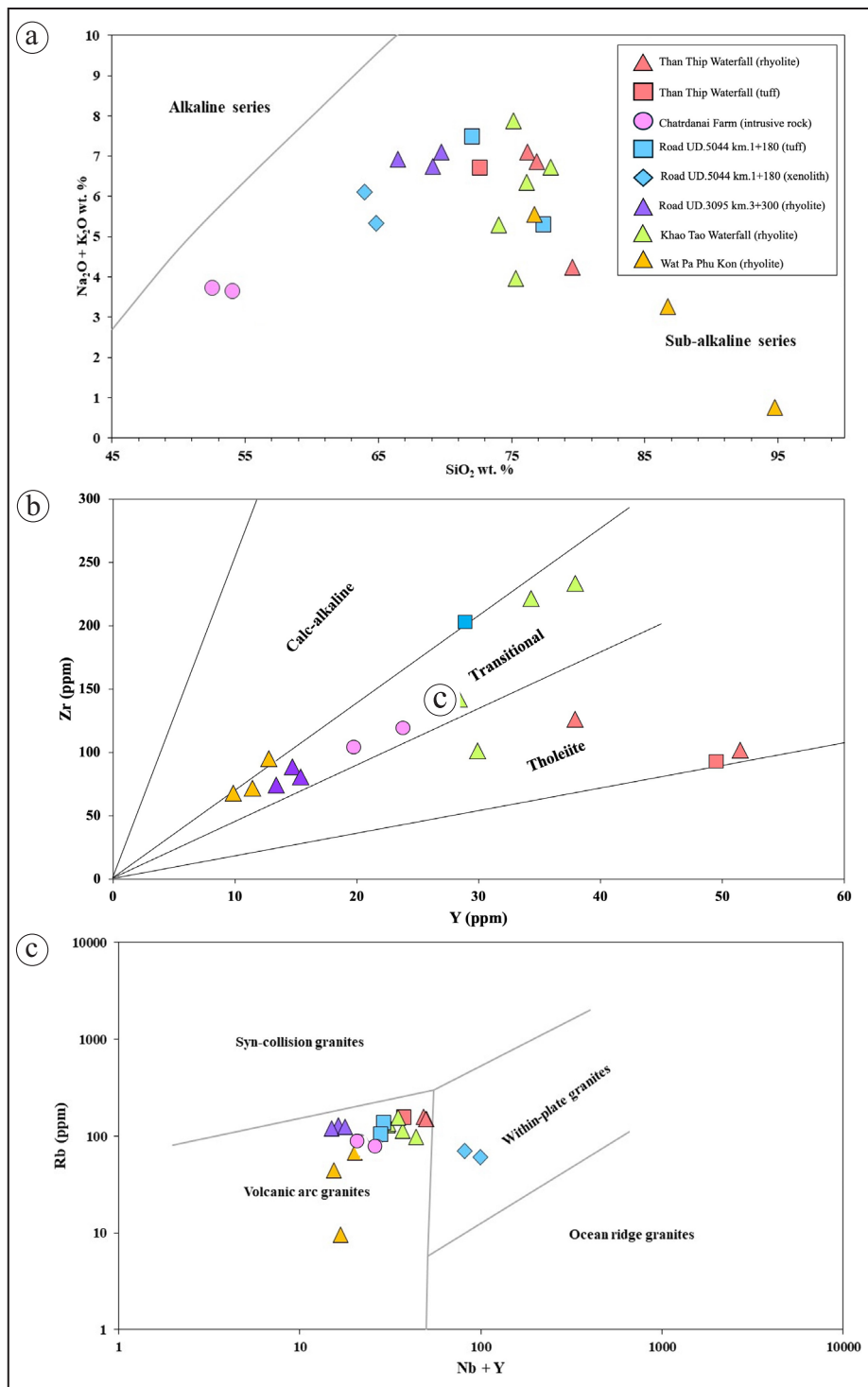


Figure 6. Diagrams of magma series and tectonic discrimination; a). $\text{Na}_2\text{O} + \text{K}_2\text{O}$ vs. SiO_2 (diagram modified from Irvine and Baragar, 1971); b). Y-Zr discrimination diagram (diagram modified from MacLean and Barrett, 1993); and c). $\text{Nb} + \text{Y}$ vs. Rb (diagram modified from Pearce *et al.*, 1984).

sure changes during volcanic eruptions (Sheikh *et al.*, 2023). These abrupt conditions hinder the complete formation of mineral crystals. Additionally, spherulites, which are primarily composed

of volcanic glass, are frequently observed within the rock. The devitrification of volcanic glass into minerals such as quartz, alkaline feldspar, and plagioclase leads to the development of fine-grained

quartz and feldspar crystals (Singtuen, 2023). At high temperatures, this devitrification process produces spherulites, lithophysae, and micro-poikilitic textures, characterized by the presence of fine-grained quartz and feldspars. Subsequent recrystallization at lower temperatures may further refine these mineral assemblages, resulting in equigranular quartz and feldspars.

The felsic volcanic rocks in this area can be categorized into three phases of eruption: (1) coherent facies, which erupted rapidly, leading to the formation of anhedral phenocrysts; (2) incoherent facies, which erupted as lava flows and preserved a eutaxitic texture; and (3) incoherent facies, which occurred during phreatic eruptions, depositing pyroclastic rocks with poorly sorted pyroclasts. In addition, fine-grained diorite (classified as basaltic andesite through geochemical analysis) exhibits an ophitic to subophitic texture, characterized by intergrowths of plagioclase and mafic minerals (hornblende and biotite). This texture supports the interpretation that these rocks formed as a shallow intrusion into the volcanic rocks. The intrusion event, or related tectonic activity, may have caused the volcanic activities in the area to undergo multiphase jointing and hydrothermal alteration, as evidenced by the presence of epidote veins and secondary alteration minerals (Kamvong and Zaw, 2009).

Geochemical analysis of major oxides and trace elements in the rock samples further supports the conclusion that the studied rocks were derived from tholeiitic (characterized by slightly elevated Zr/Y; 1.84-3.27), transitional (characterized by moderate Zr/Y; 4.84-6.60), and calc-alkaline magma series (characterized by moderately high Zr/Y; 6.97-7.15). These magmatic processes occurred in a volcanic arc tectonic setting, which was typically associated with tectonic plate collisions and subduction. The geological formations in the studied area are primarily associated with intense volcanic activity, as indicated by moderate levels of Nb+Y and Rb. However, the dacite xenoliths, particularly observed in sample NY-01, represent an exception. These xenoliths, which erupted within a plate tectonic setting character-

ized by high Nb+Y and moderate Rb levels, likely predate the formation of the surrounding volcanic arc rocks. During volcanic eruptions, these xenoliths were brought to the surface, becoming incorporated within the volcanic rocks.

Based on previous U-Pb age dating of volcanic rocks, Rb-Sr isotopic analysis suggests volcanic activity in the area occurred during the Late Devonian-Carboniferous period (Intasopa and Dunn, 1994), particularly the subduction of The Sukhothai Terrane beneath the Indochina Terrane (Intasopa and Dunn, 1994). Meanwhile, Khositanont *et al.* (2013) suggests that two samples dacite and rhyolite in Udon Thani erupted during the Silurian period (Khositanont *et al.*, 2013). In Loei-Phetchabun Volcanic Belt, the volcaniclastic rocks are associated with Silurian-Devonian fore-arc basin sediments, primarily comprising shale, tuffaceous sandstone, and limestone (Barr and Charusiri, 2011). Volcanic island arcs, which were active in the Loei and Laos regions from The Middle Devonian to The Carboniferous, played a key role in the deposition of tuffaceous sandstones and volcaniclastics (Panjasawatwong *et al.*, 2006; Long *et al.*, 2019). Volcanic arcs associated with subduction processes were active from The Late Carboniferous to The Early to Middle Permian (Salam *et al.*, 2014), likely resulting from the convergence of The Nakhon Thai Terrane and The Sibumasu Terrane with The Indochina Terrane. This tectonic interaction likely contributed to the formation of volcanic arcs in the region during this period. However, Qian *et al.* (2015) suggest that the volcanic arc in The Loei-Phetchabun Volcanic Belt was caused by the collision between The Sukhothai and Indochina Subcontinental Tectonic Plates. This collision led to the subduction of The Sukhothai Terrane beneath The Indochina Subcontinent, triggering crustal melting and subsequent volcanic eruptions (Figure 7).

Moreover, intrusive igneous rocks in the Phu Lon area, proximal to the studied site of Cafe Rai Chattanai, were dated using U-Pb isotope dating, revealing ages of 240.6 ± 1.2 million years for diorite rocks and 244 ± 4 million years for monzonite

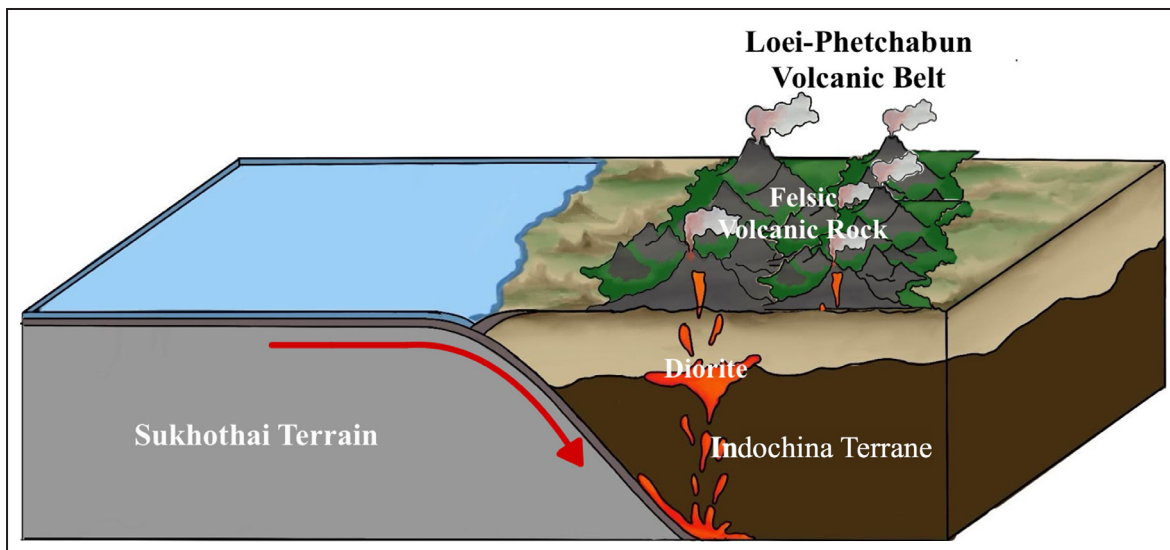


Figure 7. Tectonic model of volcanic eruption in the upper part of the Khorat Plateau, Thailand (modified from Qian *et al.*, 2015).

rocks, corresponding to the Triassic period (Nie *et al.*, 2019; Kamvong and Zaw, 2009). These formations are linked to tectonic processes associated with the collision of The Indochina Terrane and The Sibumasu Terrane, possibly representing residual magma from volcanic eruptions during the collision of the two tectonic plates and led to the intrusion and cutting of volcanic rocks in the area.

on the dominant oxides, specifically alkaline and silica content, identifying rhyolite, dacite, and basaltic andesite. Furthermore, the analysis facilitated the categorization of the magma series into three distinct types, which consist of tholeiite, transition, and calc-alkaline. The trace elements suggest that magmatic activity in the studied area occurred within a volcanic arc tectonic setting, associated with the subduction.

CONCLUSIONS

The felsic volcanic rocks of the northern Khorat Plateau can be classified into four distinct petrographic groups, each corresponding to specific volcanic facies: 1) rhyolite porphyry, 2) eutaxitic rhyolite porphyry, 3) crystal tuff, and 4) hornblende-biotite diorite. The rhyolitic rocks in this area are characterized by hollow and embayed crystals, along with the occurrence of spherulites. Some of these rocks exhibit a eutaxitic texture, indicative of lava flow, and are associated with rhyolitic tuff displaying pyroclastic texture. The mafic intrusion exhibits an ophitic signature that support it shallowly intruded into volcanic rocks. The geochemical analysis results allowed for the classification of rock types based

ACKNOWLEDGMENTS

The authors would like to acknowledge The Department of Geotechnology, Faculty of Technology, Khon Kaen University for the laboratory study. We also thank the Laboratory staff for their assistance and support during the research.

REFERENCES

Barr, S.M. and Charusiri, P., 2011. Volcanic rocks. In: Ridd, M.J., Barber, M.F., Crow, A.J. (eds.), *The Geology of Thailand*. The Geological Society, London, p.415-439.

Bas, M. L., Maitre, R. L., Streckeisen, A., & Zanettin, B., 1986. A chemical classification of

volcanic rocks based on the total alkali-silica diagram. *Journal of Petrology*, 27(3), 745-750. <https://doi.org/10.1093/petrology/27.3.745>

Boonsoong, A., Panjasawatwong, Y., and Metparsopsan, K., 2011. Petrochemistry and Tectonic Setting of Mafic Volcanic Rocks in the Chon Daen-Wang Pong Area, Phetchabun, Thailand. *Island Arc*, 20 (1), p.107-124. DOI: 10.1111/j.1440-1738.2010.00748.x

DMR, 2007. *Geology of Thailand*. Department of Mineral Resources, Ministry of Natural Resources and Environment, Thailand, 628pp.

DMR, 2009a. *Demarcation for Geological and Mineral Resources Management of Changwat Nong Khai*. Department of Mineral Resources, Ministry of Natural Resources and Environment, Thailand, 128pp.

DMR, 2009b. *Demarcation for Geological and Mineral Resources Management of Changwat Udon Thani*. Department of Mineral Resources, Ministry of Natural Resources and Environment, Thailand, 98pp.

Intasopa, S. and Dunn, T., 1994. Petrology and Sr Nd isotopic systems of the basalts and rhyolites, Loei, Thailand. *Journal of Southeast Asian Earth Sciences*, 9 (1-2), p.167-180. DOI:10.1016/0743-9547(94)90073-6

Irvine, T.N. and Baragar, W.R.A., 1971. A guide to the chemical classification of the common volcanic rocks. *Canadian journal of earth sciences*, 8 (5), p.523-548. DOI: 10.1139/e71-055

Jakes, P. and White, A.J.R., 1969. Structure of the Melanesian arcs and correlation with distribution of magma types. *Tectonophysics*, 8, p.223-236. DOI:10.1016/0040-1951(69)90099-7

Jakes, P. and White, A.J.R., 1970. K/Rb ratios of rocks from island arcs. *Geochimica et Cosmochimica Acta*, 34, p.349-356. DOI: 10.1016/0016-7037(70)90123-7

Jakes, P. and White, A.J.R., 1972. Major and trace element abundances in volcanic rocks of orogenic areas. *Bulletin of the Geological Society of America*, 83, p.29-40. DOI:10.1130/0016-7606(1972)83[29:MATEAI]2.0.CO;2

Kamvong, T. and Zaw, K., 2009. The origin and evolution of skarn-forming fluids from the Phu Lon deposit, northern Loei Fold Belt, Thailand: evidence from fluid inclusion and sulfur isotope studies. *Journal of Asian Earth Sciences*, 34 (5), p.624-633. DOI: 10.1016/j.jseaes.2008.09.004

Kamvong, T., Zaw, K., Meffre, S., Maas, R., Stein, H., and Lai, C.K., 2014. Adakites in the Truong Son and Loei fold belts, Thailand and Laos: genesis and implications for geodynamics and metallogeny. *Gondwana Research*, 26, p.165-184. DOI: 10.1016/j.gr.2013.06.011

Khositanont, S., Zaw, K., Meffre, S., Panjasawatwong, Y., Ounchanum, P., and Thanasuthipitak, Th., 2013. Geotectonic and geochronology of volcano - plutonic rocks in the Loei - Phetchabun Fold Belt. *Proceeding, The 2nd Lao-Thai Technical Conference on Geology and Mineral Resources (January 17-18, 2013)*, p.81-95.

Le Bas, M., Maitre, R.L., Streckeisen, A., and Zanettin, B., 1986. A chemical classification of volcanic rocks based on the total alkali-silica diagram. *Journal of Petrology*, 27 (3), p.745-750.

Long, Y., Zhang, D., Huang, D., Yang, X., Chen, S., and Bayless, R.C., 2019. Age composition and tectonic implications of late Ordovician–early Silurian igneous rocks of the Loei volcanic Belt, NW Laos. *International Geology Review*, 61, p.1940-1956. DOI: 10.1080/00206814.2019.1576065

MacLean W.H. and Barrett, T.J., 1993. Lithochemical techniques using immobile elements. *Journal of Geochemical Exploration*, 48, p.109-133. DOI: 10.1016/0375-6742(93)90002-4

Metcalfe, I., 2006. Palaeozoic and Mesozoic tectonic evolution and paleogeography of east Asian crustal fragments: The Korean Peninsula in context. *Gondwana Research*, 9, p.24-46. DOI: 10.1016/j.gr.2005.04.002

Metcalfe, I., 2011. Tectonic framework and Phanerozoic evolution of Sundaland. *Gondwana Research*, 19, p.3-21. DOI: 10.1016/j.gr.2010.02.016

Nie, F., Liu, S.S., Yang, Y.F., Peng, Z.M., and Guo, L.N., 2019. Zircon U-Pb dating of the

diorite of Phu Lon skarn Cu-Au deposit in Thailand and its significance. *Sedimentary Geology and Tethyan Geology*, 39 (4), p.71-78.

Nualkhao, P., Takahashi, R., Imai, A., and Charusiri, P., 2018. Petrochemistry of Granitoids Along the Loei Fold Belt, Northeastern Thailand. *Resource Geology*, 68, p.395-424. DOI: 10.1111/rge.12176

Panjasawatwong, Y., Zaw, K., Chantaramee, S., Limtrakun, P., and Pirarai, K., 2006. Geochemistry and tectonic setting of the Central Loei volcanic rocks, Pak Chom area, Loei, northeastern Thailand. *Journal of Asian Earth Sciences*, 26, p.77-90. DOI: 10.1016/j.jseae.2004.09.008

Pearce, J.A., Harris, N.B., and Tindle, A.G., 1984. Trace element discrimination diagrams for the tectonic interpretation of granitic rocks. *Journal of Petrology*, 25 (4), p.956-983. DOI: 10.1093/petrology/25.4.956

Qian, X., Feng, Q., Yang, W., Wang, Y., Chonglakmani, C., and Monjai, D., 2015. Arc-like volcanic rocks in NW Laos: Geochronological and geochemical constraints and their tectonic implications. *Journal of Asian Earth Sciences*, 98, p.342-357. DOI: 10.1016/j.jseae.2014.11.035

Salam, A., Zaw, K., Meffre, S., McPhie, J., and Lai, C.K., 2014. Geochemistry and geochronology of the Chatree epithermal gold-silver deposit: implications for the tectonic setting of the Loei Fold Belt, Central Thailand. *Gondwana Research*, 26, p.198-217. DOI: 10.1016/j.gr.2013.10.008

Sheikh, J.M., Cucciniello, C., Naik, A., Sheth, H., and Duraiswami, R., 2023. Basaltic thermal and material inputs in rhyolite petrogenesis: the Chhapariyali rhyolite dyke, Saurashtra, Deccan Traps. *Geochemistry*, 12598. DOI: 10.1016/j.chemer.2023.125984

Singtuen, V., 2023. *Igneous and Metamorphic Petrology*. Department of Geotechnology, Khon Kaen University, 70pp.

Whitney, D.L. and Evans, B.W., 2010. Abbreviations for names of rock-forming minerals. *American Mineralogist*, 95, p.185-187. DOI: 10.2138/am.2010.3371

Winchester, J.A. and Floyd, P.A., 1977. Geochemical Discrimination of Different Magma Series and Their Differentiation Product Using Immobile Elements. *Chemical Geology*, 20, p.325-343. DOI: 10.1016/0009-2541(77)90057-2

Zhao, T., Qian, X., and Feng, Q., 2016. Geochemistry, zircon U-Pb age and Hf isotopic constraints on the petrogenesis of the Silurian rhyolites in the Loei fold belt and their tectonic implications. *Journal of Earth Science*, 27, p.391-402. DOI: 10.1007/s12583-016-0671-y